NEARLY STEADY CONVECTION AND THE BOUNDARY-LAYER BUDGETS OF WATER VAPOR AND SENSIBLE HEAT

WILFRIED BRUTSAERT

School of Civil and Environmental Engineering, Cornell University, Ithaca, New York 14853, U.S.A.

(Received in final form 16 February, 1987))

Abstract. The budgets of water vapor and sensible heat in the convective atmospheric boundary (mixed) layer are analyzed by means of a simple slab approach adapted to steady large-scale advective conditions with radiation and cloud activity. The entrainment flux for sensible heat is assumed to be a linear function of the surface flux. The flux of water vapor at the top of the mixed layer is parameterized by extending the first-order Betts–Deardorff approach, i.e., by adopting linear changes for both the specific humidity and the flux across the mixed layer and across the inversion layer of finite thickness. In this way the dissimilarity of sensible heat and water vapor transport in the mixed layer can be taken into account. The experimental data were obtained from the Air Mass Transformation Experiment (AMTEX). The entrainment constant for sensible heat at the top of the mixed layer was found to have values similar to those observed in other weakly convective situations, i.e., around 0.4 to 0.6. This appears to indicate that the effect of mechanical turbulence was not negligible; however, the inclusion of this effect in the formulation did not improve the correlation. In contrast to the first-order approach, the zero-order approach, i. e., the jump equation commonly used for the flux of a scalar at the inversion, $(\overline{w'c'})_h = w_e \Delta c$ (where w_e is the entrainment velocity and Δc the concentration jump across the inversion), was found to be invalid and incapable of describing the data.

1. Introduction

The convective boundary layer has mostly been considered in the context of the unsteady heating process in the course of a sunny day over a uniform surface. The temperature profile of such a boundary layer is generally characterized by a superadiabatic gradient in the relatively shallow sublayer near the surface, and an adiabatic to often slightly subadiabatic gradient in the relatively thick well-mixed layer higher up; the boundary layer is typically capped by a well-defined inversion, i.e., a layer with a very stable temperature gradient. Above this inversion the temperature profile exhibits a less stable gradient, which remains practically unaffected by the underlying surface and which is conditioned primarily by the general circulation pattern. The profile of the specific humidity is generally similar to that of the potential temperature in the surface sublayer. However, this is not the case in the mixed layer and through the temperature inversion lid; as pointed out already by Mahrt (1976), the specific humidity typically decreases somewhat with elevation in the mixed layer, and it displays a sharp drop across the inversion layer. An example of this is given in Figure 1.

The uniform temperature profile in the mixed layer is the result of the convective activity of unstable air, and of the entrainment of some warmer air downward from the overlying inversion. The entrained air is also dry, which accounts for the observed humidity gradient in the mixed layer. The mixing occurs partly as ordered motion with some coherent structure in the form of more or less discrete convective elements, i.e.,

Boundary-Layer Meteorology **39** (1987) 283–300.

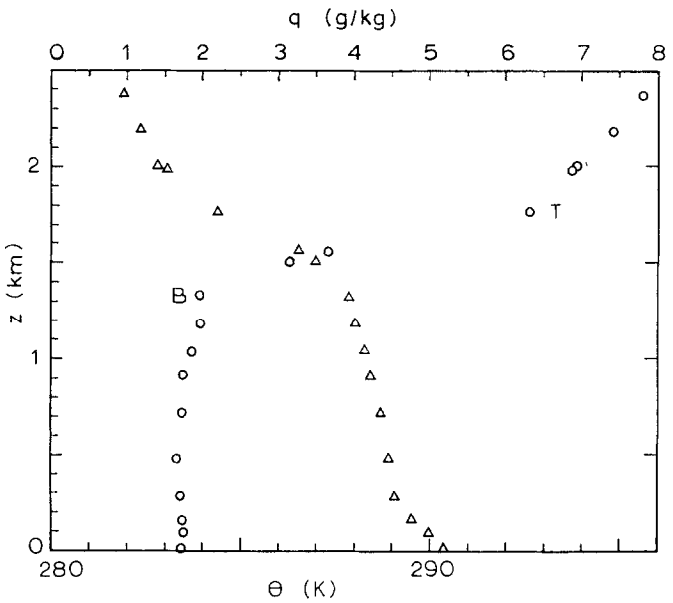

Fig. 1. Example of the profiles of mean potential temperature (circles) and specific humidity (triangles) during AMTEX at the Keifu station (February 16, 1975; 21 : 00) *B* is the bottom and *T* the top of the inversion.

rising plumes or thermals, which penetrate by 'overshooting' into the inversion; this penetration by the plumes causes some mixing with the overlying warmer air and this is one of the main mechanisms of the entrainment of the warmer air down into the boundary layer. These upward moving plumes are balanced by a downdraft of air over a somewhat wider area. Observations by Lenschow and Stephens (1980) in the experimental area of AMTEX have revealed that thermals occupy about 20 to 30% of the record along an aircraft flight path. Other measurements, regarding thermals and their structure, have been reported by Kaimal *et al.* (1976), Manton (1977), Coulman (1978), Grossman (1982), and Taconet and Weill (1983). The role of thermals in the overall transport mechanisms in the mixed layer and through the inversion is gradually being clarified (e.g., Mahrt and Paumier, 1984).

In spite of the complexity of the convective boundary layer, in the past it has been possible to describe the transport of scalar admixtures in it by simple 'slab' and 'jump' models, and to obtain some very useful results. In the slab approximation, the boundary layer is assumed to have a vertically uniform concentration of the admixture, with the exception of a negligibly thin layer near the surface. In the jump approximation to express entrainment, the capping inversion is assumed to be so thin, that it can be taken as a sharp discontinuity in concentration, which separates the uniformly mixed layer below from the stable, warmer and drier air of the free atmosphere above. This approach was introduced by Lilly (1968) in the case of potential temperature. It was subsequently realized that in many situations the vertical thickness of the inversion layer is not

negligible and that it may sometimes even be comparable to that of the underlying mixed layer. This was indicated by Betts (1974), who devised a simple first-order model for an inversion layer of finite thickness with a linear temperature change across it; the approach was restricted, however, by the assumptions that the inversion thickness and the temperature difference across it are constants. The first-order model was improved by Deardorff (1979) by eliminating the need for these two assumptions; but since he felt the first-order to be deficient, he then proposed a further extension involving a more realistic thermal structure within the inversion layer. So far, none of these improvements on the original jump approach has been tested with field data.

In this paper an analysis is given of the budgets of sensible heat and water vapor in a convective atmospheric boundary layer; the situation under consideration is the result primarily of large-scale, close to steady advection of relatively cold, dry air over relatively warm water. The experimental data were obtained during the Air Mass Transformation Experiment (AMTEX) which took place in February 1975 in the East China Sea. The budget analysis is performed on the basis of the simple slab approach adapted for this purpose. The entrainment of sensible heat at the inversion is treated in the way suggested by Carson (1973a), Tennekes (1973), and Driedonks (1982). The entrainment flux of water vapor is dealt with by means of an extension of the first-order approach to specific humidity; in the process it will be shown that this approach involving linear profiles of the humidity, of the temperature and of the corresponding fluxes, leads to more realistic results with the present data than the zero-order jump approximation.

2. Slab Approach with Cloud Activity and Radiation

2.1. Potential Temperature

The formulation of the equation for potential temperature given here follows in general the earlier work of Ball (1960), Lilly (1968), Carson (1973a), and others; however, a somewhat different account is taken of large-scale advection, cloud activity, and radiation.

In and near the atmospheric boundary layer, the Reynolds equation for conservation of enthalpy can be written as

$$\frac{\partial \theta}{\partial t} + V \cdot \nabla_{xy} \theta + w \frac{\partial \theta}{\partial z} = -\frac{\partial}{\partial z}(\overline{w'\theta'}) - \frac{1}{\rho c_p} \frac{\partial F_R}{\partial z} + \frac{l_c}{\rho c_p}, \tag{1}$$

where θ is the mean (in the turbulence sense) potential temperature, θ' the turbulent fluctuation, V and w the mean (in the turbulence sense) horizontal and vertical velocity, ∇_{xy} the horizontal gradient, z the vertical coordinate, w' the vertical turbulent velocity, ρ the density of the air, c_p the specific heat at constant pressure, F_R the radiative heat flux and l_c the point heat source stemming from water vapor condensation.

The boundary layer is assumed to be a slab of thickness h with constant horizontal velocity (V = const.) and constant potential temperature (θ = const.). Integration of (1)

between $z = 0$ and $z = h$, produces immediately (to a close approximation for the last two terms)

$$h\left(\frac{\partial}{\partial t} + V \cdot \nabla_{xy}\right)\theta = \frac{H}{\rho_0 c_p} - (\overline{w'\theta'})_h - (Q_R - L_c)/\rho_0 c_p\,, \tag{2}$$

where ρ_0 is the density of the air near the water surface $z = 0$, H the turbulent flux of sensible heat at the surface, $(\overline{w'\theta'})_h$ the turbulent flux of potential temperature at the top of the boundary layer $z = h$, $Q_R = (F_R)_h - (F_R)_0$ the heat loss rate by radiative of cooling from the entire boundary layer and L_c the rate at which heat is gained by condensation and cloud formation over the entire boundary layer.

In many applications of the slab approach to strongly convective situations, it has been found to be convenient (e.g., Betts, 1973; Carson, 1973a; Tennekes, 1973) to parameterize the turbulent flux at $z = h$ in terms of that at $z = 0$, as follows

$$(\overline{w'\theta'})_h = -A(H/\rho_0 c_p)\,, \tag{3}$$

where A may be called the entrainment constant. Equation (3) was already implicit in the studies of Ball (1960) and Lilly (1968) who adopted $A = 1$ and $A = 0$, respectively. Carson (1973b) suggested that A may vary throughout the different phases of boundary-layer development but that experimental evidence favors an average of 0.25; Tennekes (1973) proposed $A = 0.2$. Subsequent work (e.g., Stull, 1976; Heidt, 1977) has confirmed that A covers a range from 0.1 to 0.4 with most of the experimentally determined values lying between 0.2 and 0.3. Artaz and André (1980), who compared different models for the mixed layer, concluded that the simplest one based on (3) with constant A, performed at least as well as other more complicated ones. Still, there are indications that A is larger under weakly convective conditions. Dubloscard (1980), who analyzed morning convection situations, found that A is larger for smaller values of H; the mean was around $A = 0.58$ with a range between 0.2 and 1.0.

When the convective activity is relatively weak, the turbulent transport at $z = h$ involves also mechanical entrainment, which is affected by the shear stress in the boundary layer. For such conditions, Tennekes (1973) proposed an interpolation formula taken as the weighted sum of (3) and an expression obtained by Kato and Phillips (1969) for the rate of entrainment at the oceanic thermocline; this can be written as

$$-(\overline{w'\theta'})_h = A(H/\rho_0 c_p) + BT_0 u_*^3/(gh)\,, \tag{4}$$

where $u_* = (\tau_0/\rho)^{1/2}$ is the friction velocity, τ_0 the surface shear stress, T_0 a reference temperature and g the acceleration of gravity. Later Driedonks (1982) confirmed that (4) with $B = 5$ (after the laboratory experiments of Kantha *et al.*, 1977) and $A = 0.2$, gave indeed better results in describing the boundary-layer development than (3) for the early morning hours. For conciseness of notation, (4) can be written as

$$-(\overline{w'\theta'})_h = \frac{A}{\rho_0 c_p}\left(H + \frac{B}{A}M\right), \tag{4'}$$

where by definition $M = \rho_0 c_p T_0 u_*^3/(gh)$, which reflects the effect of mechanical entrainment.

2.2. Specific humidity

The equation for the mean specific humidity in a slab model can be derived in a way similar to that for the potential temperature. Again, in and near the boundary layer, the Reynolds equation for water vapor is

$$\frac{\partial q}{\partial t} + V \cdot \nabla_{xy} q + w \frac{\partial q}{\partial z} = -\frac{\partial}{\partial z}(\overline{w'q'}) - \frac{l_c}{\rho L_e}, \tag{5}$$

where q is the mean (in the sense of turbulence) specific humidity, q' the turbulent fluctuation, and L_e the latent heat of vaporization.

Integration of (5) across the boundary layer as a slab of thickness h, with constant velocity V, constant divergence $\nabla_{xy} \cdot V$ (implying that w is proportional to z), and variable q, produces

$$h\left(\frac{\partial}{\partial t} + V \cdot \nabla_{xy}\right) q_a + w_e(q_a - q_h) = E/\rho_0 - (\overline{w'q'})_h - L_c/(\rho_0 L_e), \tag{6}$$

where E is the rate of evaporation at the surface, q_a the vertical mean of q and $(\overline{w'q'})_h$ the turbulent flux of specific humidity at the top of the mixed layer; w_e is defined by

$$w_e = \left(\frac{\partial}{\partial t} + V \cdot \nabla_{xy}\right) h - w_h \tag{7}$$

and is called the entrainment velocity, because $-w_e$ represents the vertical velocity of fluid relative to the upper boundary of the mixed layer. Unlike $(\overline{w'\theta'})_h$ with (3) or (4), no simple parameterizations are available for $(\overline{w'q'})_h$. This matter will be dealt with in Section 3. The second term on the left-hand side in (6) is usually small, so that the slab approximation of the mixed layer may also be adopted for humidity; in what follows this term is neglected.

2.3. Elimination of condensation term

In the present paper, convection is considered under nearly steady conditions; thus for brevity of notation in what follows, the term $\partial/\partial t$ is dropped, with the understanding that it can be reinserted if needed. Also the xy subscript is dropped, so that ∇ denotes the horizontal gradient.

The condensation source term L_c is not easily determined; it can be eliminated by adding the two slab equations (2) and (6), viz.,

$$\rho_0 h(c_p V \cdot \nabla\theta + L_e V \cdot \nabla q_a) + Q_R = H - \rho_0 c_p (\overline{w'\theta'})_h + LE - \rho_0 L_e (\overline{w'q'})_h, \tag{8}$$

where $LE = L_e E$ is the surface flux of latent heat.

3. Water Vapor Flux at the Top of the Mixed Layer

Several simple expressions, such as (3) and (4), are available to parameterize $(\overline{w'\theta'})_h$, the sensible heat flux of entrainment into the mixed layer. These and other more complex expressions that have appeared in the literature were derived at mostly from considerations of the turbulent kinetic energy burget. Because water vapor is a more passive scalar than sensible heat, a different approach is necessary.

3.1. Proposed first-order model for water vapor

The first-order approach was introduced for sensible heat by Betts (1974) and then further worked out with fewer restrictions by Deardorff (1979). The main features of their model are shown in Figure 2. In brief, the potential temperature is constant in the

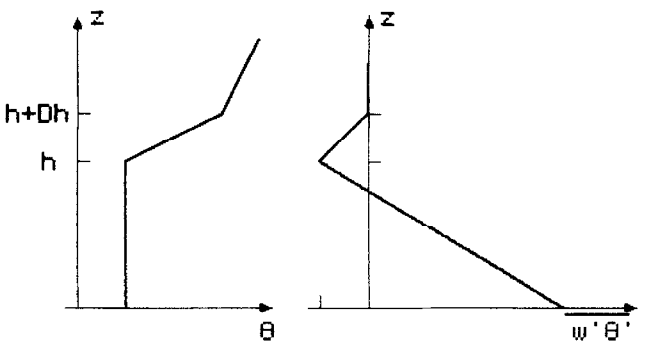

Fig. 2. Profiles of the potential temperature θ and of the turbulent flux $(\overline{w'\theta'})$ for the first-order model.

mixed layer, but it is subject to linear changes with height across the inversion layer of thickness Δh and above it in the free atmosphere. The turbulent flux $(\overline{w'\theta'})$ undergoes linear changes with height in the mixed layer and through the inversion.

This approach, involving linear segments for the profiles of concentration and flux, can be extended to water vapor as shown in Figure 3. The specific humidity is not

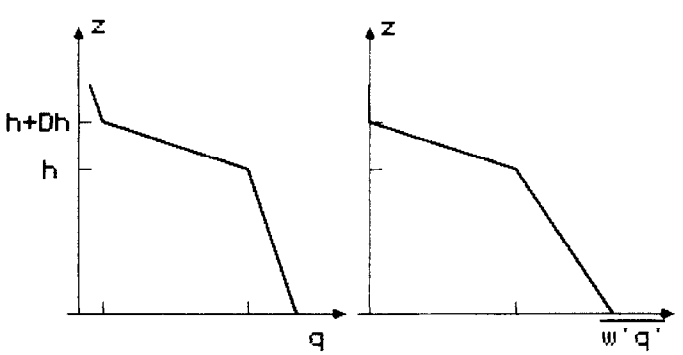

Fig. 3. Profiles of the specific humidity q and of the water vapor flux $(\overline{w'q'})$ for the first-order model.

constant inside the mixed layer but it changes linearly between q_0 and q_h; across the inversion the change is Δq. The turbulent flux decreases linearly with height from a value of (E/ρ_0) at $z = 0$ to a positive value $(\overline{w'q'})_h$ at $z = h$; above $z = h$ it decreases linearly to zero at the top of the inversion where $z = h + \Delta h$.

The entrainment of dry air into the mixed layer can be derived by applying Deardorff's (1979) suggestion at $z = h$. Thus q and $(\overline{w'q'})$ are assumed to be sufficiently smooth around h to allow differentiation of (5) with respect to z; subsequent integration between $h - \varepsilon$ and $h + \varepsilon$, where ε is a small value, and neglect of l_c, i.e.,

$$\int_{h-\varepsilon}^{h+\varepsilon} \left[\frac{\partial}{\partial z}\left(\frac{\partial}{\partial t} + V\cdot\nabla \right) q + \frac{\partial}{\partial z}\left(w \frac{\partial q}{\partial z} \right) \right] \mathrm{d}z = - \int_{h-\varepsilon}^{h+\varepsilon} \frac{\partial^2}{\partial z^2} (\overline{w'q'})\, \mathrm{d}z$$

yields with Leibniz's rule, when ε approaches zero,

$$(\Delta q - s\,\Delta h) w_e = \alpha(E/\rho_0) - (1 + \alpha)(\overline{w'q'})_h , \tag{9}$$

where $s = \partial q/\partial z$ is the gradient in the mixed layer, w_e is defined in (7), and $\alpha = \Delta h/h$.

In the present context, w_e is unwelcome because it is not easily determined; it can be eliminated by considering the analog of (9) for sensible heat. This is

$$(\Delta\theta - \gamma_a \Delta h) w_e = \alpha H/(\rho_0 c_p) - (1 + \alpha)(\overline{w'\theta'})_h , \tag{10}$$

where $\gamma_a (= \partial\theta/\partial z)$ is the mean gradient of the potential temperature in the mixed layer; because the temperature in the mixed layer is nearly constant, this term is usually negligible. Equation (10) with $\gamma_a = 0$ is the same as Deardorff's (1979; (9)) result, but his definition of w_e is slightly different. At any rate, combination of (9) and (10) produces the main result

$$(\overline{w'q'})_h = \beta E/\rho_0 - \frac{(\Delta q - s\,\Delta h)}{\Delta\theta} [\beta H/(\rho_0 c_p) - (\overline{w'\theta'})_h] , \tag{11}$$

where $\beta = \Delta h/(h + \Delta h)$. With available parameterizations for $(\overline{w'\theta'})_h$ such as (3) and (4), it is possible to calculate the water vapor flux from surface fluxes and profile characteristics of θ and q. If $(\overline{w'\theta'})_h$ is determined by means of (3), the result is

$$(\overline{w'q'})_h = \beta E/\rho_0 - \frac{(\Delta q - s\,\Delta h)}{\Delta\theta} (\beta + A_1) H/(\rho_0 c_p) . \tag{12}$$

In the case of Tennekes's (1973) interpolation formula, (4) or (4′), the result is

$$(\overline{w'q'})_h = \beta E/\rho_0 - \frac{\Delta q - s\,\Delta h}{\Delta\theta} [\beta H/(\rho_0 c_p) + \\ + A_2(H + BM/A)/(\rho_0 c_p)] . \tag{13}$$

The constants A_1 and A_2 represent A in the substitutions of (3) and (4), but the subscripts have been added to allow for the approximations in the first-order model; in the data

analyses, therefore, A_1 and A_2 may be different from A. The assumption that B/A is the same is not necessarily valid, but because in convective situations BM/A is usually small, this may be an acceptable approximation.

3.2. Zero-order model for water vapor

The entrainment in the zero-order approach can be derived by integrating (1) and (5) from $z = h$ to $z = h + \Delta h$, and then allowing Δh to approach zero. The inversion flux $(\overline{w'q'})_h$ can also be obtained directly from the first-order result (9) by letting $\Delta h = 0$. This gives

$$(\overline{w'q'})_h = w_e \Delta q . \tag{14}$$

Similarly, from (10)

$$(\overline{w'\theta'})_h = w_e \Delta\theta . \tag{15}$$

Thus from (14) and (15)

$$(\overline{w'q'})_h = (\overline{w'\theta'})_h \Delta q/\Delta\theta . \tag{16}$$

If $(\overline{w'\theta'})_h$ is parameterized by means of (3), this becomes in terms of the surface heat flux

$$(\overline{w'q'})_h = -A_3(H/\rho_0 c_p)\Delta q/\Delta\theta . \tag{17}$$

If (4′) is used, (16) becomes

$$(\overline{w'q'})_h = A_4[(H + BM/A)/(\rho_0 c_p)]\Delta q/\Delta\theta . \tag{18}$$

Again, the constants A_3 and A_4 have been given a subscript to allow for the possibility that they are different from A.

It can be seen that $c_p(\overline{w'\theta'})_h/L_e(\overline{w'q'})_h$ may be considered a kind of Bowen ratio for the turbulent transport at the bottom of the inversion. By virtue of (14), the ratio of the fluxes equals $\Delta\theta/\Delta q$. Within the context of K-theory, this means that the zero-order jump approach is somewhat analogous with the assumption that at the inversion, the eddy diffusivities for sensible heat, K_H, and for water vapor, K_E, are exactly the same.

4. The Experimental Data

The second phase of the Air Mass Transformation Experiment (AMTEX), which was carried out in the East China Sea over an area with center at Okinawa in the second half of February in 1975, provided the data. General descriptions of this experiment have been given by among others Lenschow and Agee (1974, 1976) and Ninomiya (1974, 1977). One of the objectives was to study the large-scale advection of relatively cold and dry air off the Asian Continent onto the relatively warm water surface of the East China Sea. When this situation prevails, the wind direction is typically northwest to north and the temperature and vapor pressure distributions in the air are characterized by more or less straight and parallel iso-lines more or less orthogonal to the wind and with a spacing of the order of 1 to 2 °C/100 km and 1 to 2 mb/100 km, respectively.

To avoid local nonhomogeneities and disturbances of the boundary layer, the analysis was carried out with data from three stationary research vessels (rather than from island stations); these were the Ryofu-Maru located near 29.5 N, 127.3 E, the Keifu-Maru near 28.0 N, 125.0 E, and the Nojima near 23.4 N, 127.9 E. Also to avoid other possible boundary-layer disturbances, data were not used whenever measurable precipitation took place or whenever the relative humidity was at 100% over a significant portion of the atmospheric boundary layer. (This is the main reason why the 1974 data were not used.) Similarly, data for negative or uncertain advection (which may preclude convective conditions), or for negative surface fluxes were eliminated. Over the ocean surface, the diurnal cycle is usually quite weak and barely noticeable. Therefore, the data were averaged on a daily basis. This did not completely eliminate the unsteadiness from the data. Still, the magnitude of the $\partial T/\partial t$ terms was usually around 10% of that of the corresponding $V \cdot \nabla T$ terms (see Table I) which is probably smaller than the error of the advective terms; the same was true for the specific humidity. Because in contrast to the other terms in (6), the $\partial/\partial t$ terms are not systematically positive or negative, it was felt that for the present analysis they may be considered as random noise. The elimination of the unsuitable data left for each of the variables a set of 31 daily average data points for the analysis. The dates of these days for the three ships are shown in Table I. The raw data used to derive the needed variables have been published as AMTEX '75 Data Reports at the Meteorological Research Institute, Koenji, Suginami in Tokyo. Figure 4 shows the general area of AMTEX with the positions of the three research ships.

In (8) the advection terms drive the boundary layer. To calculate these terms, the near-surface horizontal gradients were determined as follows. Daily average maps were made for the East China Sea showing isotherms for near-surface (at 10 m above sea-level) air temperature and isobars of near-surface vapor pressure. These were made on the basis of all available data from the research vessels (3-hourly) and small islands (3-hourly), buoys, fishing vessels and other 'ships of opportunity', and also from well-exposed near-shore continental stations. An example of the mean temperature and vapor pressure distribution is shown in Figure 4. The values of the gradients were then multiplied by the corresponding wind velocity components in the direction of the gradients to obtain the values listed in Table I, viz., $V_0 \cdot \nabla T_0$ and $V_0 \cdot \nabla e_0$, where V_0 is the near-surface wind velocity vector, T_0 the near-surface air temperature, and e_0 the near-surface vapor pressure. (The daily mean values for wind direction have already been given by Kondo, 1977.) The wind velocity at 10 m may be considered a good estimate of the mean wind in the convective boundary layer (e.g., Kondo, 1977, Figures 6 and 7 for Keifu); the same is true for potential temperature at 10 m and the mean in the boundary layer (e.g., Figure 1). Therefore, it may be assumed that

$$V \cdot \nabla \theta = V_0 \cdot \nabla T_0 \,. \tag{19}$$

The same cannot be said about the specific humidity. As can be seen in Figure 1, q is not uniform across the boundary layer. However, the horizontal gradient of $q = (0.622e/p)$ obtained from the maps is for the near-surface value q_0, rather than for the mean q_a as required for the analysis. Therefore, it was assumed that the advective

TABLE I

Daily mean values

No.	Date	T_0 (°C)	h (m)	Δh (m)	$V_0 \cdot \nabla T_0$ 10^{-5} °C s^{-1}	$V_0 \cdot \nabla e_0$ 10^{-5} mb s^{-1}	f (%)	$-s$ 10^{-6} g/(g m)	$\Delta\theta$ (°C)	$-\Delta q$ 10^{-4} g/g	Q_R Wm^{-2}
					Ryofu (29.5 N, 127.3 E)						
1	15 Feb., 1975	11.2	1240	220	16.7	14.3	71	1.30	2.9	13.3	27
2	16 Feb., 1975	9.9	1550	725	13.5	7.37	77	1.09	9.4	18.2	33
3	17 Feb., 1975	10.3	1617	462	8.72	4.42	80	0.76	6.6	19.7	33
4	18 Feb., 1975	11.9	1510	200	8.96	4.44	83	0.87	3.6	12.4	32
5	19 Feb., 1975	9.1	1400	325	14.0	5.87	82	0.95	4.0	18.3	30
6	22 Feb., 1975	7.5	1983	477	16.2	12.2	71	0.95	8.4	7.6	36
7	23 Feb., 1975	9.4	1555	355	8.69	3.58	80	0.67	5.5	14.6	33
8	26 Feb., 1975	14.6	845	430	8.27	6.11	90	1.55	4.3	25.3	14
9	28 Feb., 1975	10.8	1117	812	11.1	6.06	88	0.95	10.7	26.4	24
					Keifu (28.0 N, 125.0 E)						
10	15 Feb., 1975	11.4	1457	770	17.2	12.8	75	1.43	9.7	19.4	31
11	16 Feb., 1975	10.5	1357	583	13.1	5.19	81	0.89	9.4	22.7	29
12	17 Feb., 1975	11.3	1462	403	6.12	4.17	81	0.69	7.4	17.4	31
13	18 Feb., 1975	12.4	1332	245	13.0	5.45	81	1.01	3.4	20.5	29
14	19 Feb., 1975	10.3	1220	483	15.4	5.89	77	0.64	5.4	19.7	26
15	20 Feb., 1975	9.8	1367	303	15.1	9.46	74	1.07	2.8	6.6	30
16	21 Feb., 1975	7.7	1645	455	16.9	14.8	70	0.71	6.3	8.2	34
17	22 Feb., 1975	8.5	1757	597	17.6	10.7	70	0.73	11.0	9.0	35
18	23 Feb., 1975	9.8	1147	415	3.37	2.64	85	0.93	4.9	18.0	24
19	26 Feb., 1975	16.2	602	462	6.13	4.78	90	1.63	3.8	8.4	8
20	28 Feb., 1975	11.6	652	950	8.12	5.23	86	1.66	9.1	16.9	9
					Nojima (23.4 N, 127.9 E)						
21	15 Feb., 1975	19.6	1685	665	9.62	15.7	81	1.30	9.8	47.0	34
22	16 Feb., 1975	17.9	1965	307	7.47	17.9	77	1.16	7.6	22.2	36
23	17 Feb., 1975	18.5	1627	440	4.86	3.69	81	1.00	5.8	4.7	33
24	18 Feb., 1975	19.0	2467	250	3.81	6.60	77	1.40	2.4	2.7	38
25	19 Feb., 1975	17.5	1690	310	7.48	14.2	78	1.98	4.4	17.1	34
26	20 Feb., 1975	17.5	1600	300	9.46	10.9	79	1.57	5.0	25.8	33
27	21 Feb., 1975	15.6	1915	447	11.7	12.3	73	0.77	11.7	23.0	36
28	22 Feb., 1975	16.0	2090	347	13.6	12.1	71	1.02	10.1	11.8	36
29	23 Feb., 1975	16.7	1920	635	7.14	8.29	74	1.27	9.9	18.7	36
30	24 Feb., 1975	19.4	1975	525	2.95	1.76	71	1.16	5.9	4.0	36
31	28 Feb., 1975	19.6	1220	465	5.78	7.22	87	1.83	4.2	27.7	26
Average		13.3	1515	463	10.4	8.26	79	1.13	6.6	17.0	29.9

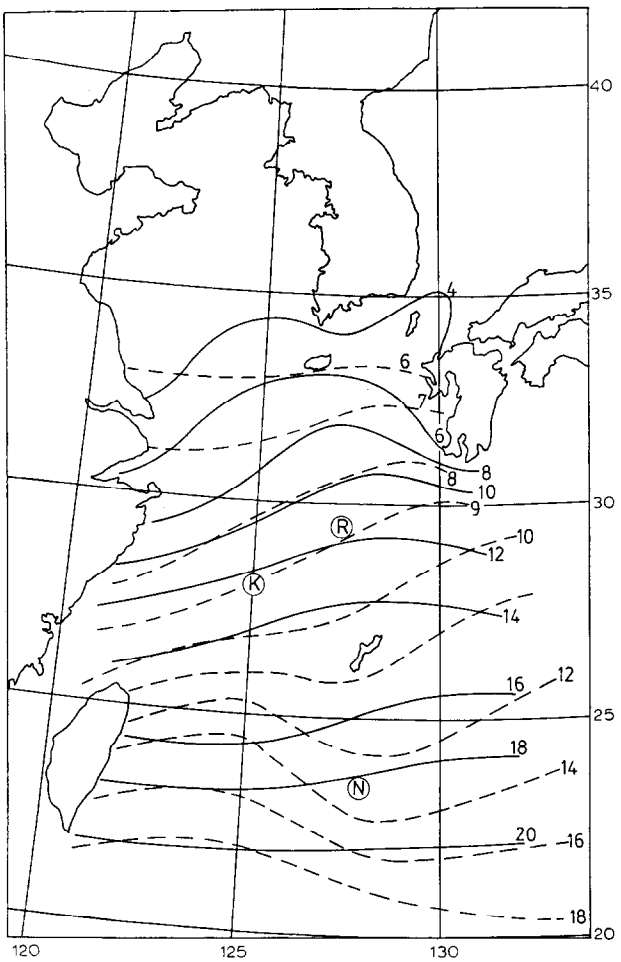

Fig. 4. Map of the AMTEX area with the location of the stationary research vessels Ryofu (R), Keifu (K), and Nojima (N). As an illustration, the mean daily isotherms of T_0 in °C (solid lines) and the mean daily isobars of e_0 in mb (dashed lines) are shown for February 18, 1975.

boundary layer exhibits self-similarity or self-preservation in the distribution of the humidity with elevation, so that it may be assumed that

$$V \cdot \nabla q_a = f(0.622/p_0) V_0 \cdot \nabla e_0 , \tag{20}$$

where by definition $f = (q_a/q_0)$ is the ratio of average over near-surface value of q. Because it was found that the estimate $f = (q_0 q_h)^{1/2}/q_0$ was usually within 1 or 2% of the true f obtained by integration over the whole profile, these are the values given in Table I.

The vertical profiles of temperature and specific humidity were obtained from the radiosonde measurements (pressure, temperature, and relative humidity) which had

been made four times daily, except only twice daily on the Nojima during the second week of AMTEX 75. For each ascent, the height of the mixed layer h, i.e., the bottom of the inversion, was determined as the lowest level where $dT/dp \leq 4\ ^\circ C/100$ mb. The h values given in Table I are the daily means. The top of the inversion, where $z = h + \Delta h$, was determined as the level where again $dT/dp > 4\ ^\circ C/100$ mb. The values of q_h, the specific humidity at $z = h$, were obtained from the profiles and used in the calculation of f. The vertical gradients of specific humidity in the mixed layer s ($= \partial q/\partial z$) were obtained by linear regression of the q-profiles in the mixed layer. These values of Δh, f, and s, together with those of the strength of the inversion, as expressed by the change in potential temperature $\Delta\theta$, and specific humidity Δq, are given as averages for each day in Table I. The values of the near surface air temperature T_0, given in Table I, were taken as the mean of the three-hourly measurements at 10 m above the water surface.

TABLE II

Means (over 31 data points) of some energy and vapor budget terms of the boundary layer (W m^{-2})

$\rho_0 h c_p V \cdot \nabla\theta$	$\rho_0 h L_e V \cdot \nabla q_a$	H	LE	$M = \rho_0 c_p T_0 u_*^3/(gh)$
195.4	187.0	116.9	352.5	1.428

The radiative cooling rate term Q_R can be calculated from a knowledge of the temperature and humidity profiles in the atmosphere and of the amount and type of cloudiness. Such calculations were performed by Nitta (1976) for 1974 over the

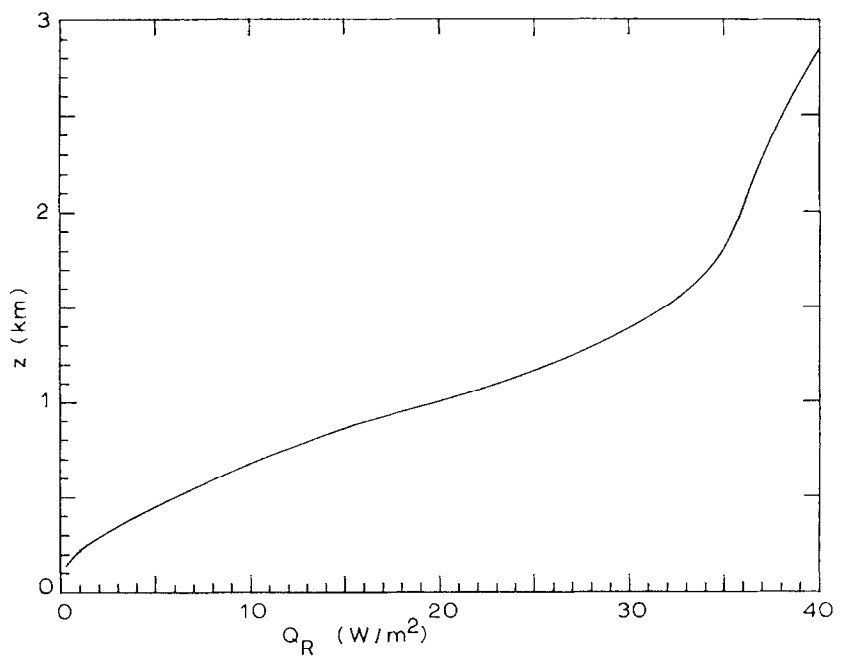

Fig. 5. Radiative cooling rate of entire boundary layer as function of its thickness. The curve was derived as an average profile from Nitta's (1976) calculations for the cold air outbreak 24–28 February, 1974.

AMTEX area, on the basis of area-averaged profiles and cloud-information; however, the calculation process and the data compilation is tedious. As Q_R is a minor term compared to the others (see Tables I and II), it was decided to use an approximate procedure. This consisted of determining Q_R as the average integral of the radiative cooling profiles calculated by Nitta (1976, Figure 6) as a function of elevation over the period February 24–28, 1974. A similar procedure had already been used by Murty (1976) on the basis of the entire AMTEX 74 period. In the present study, the average was taken only over the shorter 5-day period, because it was a cold-air outbreak, which resembled more closely the conditions of AMTEX 75. The resulting Q_R profile which was obtained on the basis of Nitta's (personal communication) numerical results is given in Figure 5. Thus it is assumed that Q_R is a function only of boundary-layer thickness. The values of Q_R derived from Figure 5 for each day and ship station are given in Table I.

The daily values of the surface fluxes of sensible heat H, of water vapor E and of momentum u_* have been calculated by Kondo (1976, 1977) by means of a bulk transfer method for diabatic conditions and variable roughness of the sea surface. These data need not be presented here, but their averages for the 31 days of the present study are $H = 116.9\ \mathrm{W\ m^{-2}}$, $LE = 352.5\ \mathrm{W\ m^{-2}}$, and $u_* = 0.366\ \mathrm{m\ s^{-1}}$. (See also Table II.)

5. Analysis of the Data

The data were analyzed in the framework of the first-order model application developed herein. They were subjected to linear regression analysis through the origin, by means of the following equation in standard notation

$$X_1 = a_{12}X_2 + a_{13}X_3 . \tag{21}$$

In the case of the simplest entrainment relation for sensible heat, i.e., (3),

TABLE III

Results of regression analyses for first-order model with Equations (8), (3), and (12)

Data	$A(\pm\sigma)$	$A_1(\pm\sigma)$	Correlation coefficients		
			Multiple	Partial	
			$R_{1.23}$	$R_{12.3}$	$R_{13.2}$
Ryofu and Keifu	0.40 (±0.17)	0.78 (±0.31)	0.84	0.83	0.44
All 3 ships	0.39 (±0.26)	0.39 (±0.49)	0.48	0.48	0.21
All data w/out No. 21	0.43 (±0.23)	0.57 (±0.44)	0.58	0.58	0.27
Ryofu and Keifu if $Q_R = 0$	0.25 (±0.17)	0.84 (±0.31)	0.82	0.82	0.45
Ryofu and Keifu if $s = 0$	0.57 (±0.20)	0.76 (±0.29)	0.83	0.83	0.44

Note: σ denotes standard error of the regression coefficient.

Equation (21) represents (8) with (3) and (12); thus the variables are $X_1 = \rho_0 h(c_p V \cdot \nabla\theta + L_e V \cdot \nabla q_a) + Q_R - LE(1-\beta) - (\Delta q - s\,\Delta h)\beta L_e H/(\Delta\theta\, c_p)$, $X_2 = H$ and $X_3 = (\Delta q - s\,\Delta h)L_e H/(\Delta\theta\, c_p)$ and the regression constants are $a_{12} = 1 + A$ and $a_{13} = A_1$. The results and the correlation coefficients are shown in Table III. The horizontal gradients in the vicinity of the Nojima were not easy to determine mainly because of the relative scarcity of surface measurements and of the proximity of the Kuroshio so that these data are probably less reliable. Therefore, the results are given separately for the data of Ryofu and Keifu, and then for the data of all three ships.

It can be seen that the entrainment constant $A = 0.4$ lies in the general range of values reported previously in the literature. The entrainment constant A_1 appears to be about twice as large for Ryofu and Keifu, based on the most reliable data, and the same, i.e., $A_1 = 0.4$ for all data including Nojima. Ideally, A_1 should be equal to A; in view of the overlapping standard errors of A_1 and A, there is no reason to conclude that they are different.

To test the sensitivity of these results further, the data were also analyzed by running the regression with all the data, except No. 21 (February 15, 1975 of Nojima, see Table I), which for some reason seems to be particularly out of line. As shown in Table III, without this one data point, A_1 is still close to A but the correlation coefficients have improved considerably. This supports the above conclusion that A_1 is not different from A. The effect of radiation was considered in the analysis, by putting $Q_R = 0$ in (8). The results in Table III show that this makes A_1 quite different from A. Also, the omission of radiation has reduced the correlations somewhat. This suggests that while Q_R is a minor term in the equation, it is probably not negligible. Finally, the data were also analyzed by assuming that the specific humidity is uniform in the boundary layer so that s may be taken as zero in (12). It can be seen in Table III that this assumption did not affect the results very much. The correlations appear to be slightly smaller, but A_1 is closer to A than when s in included.

The heating rate in the advective boundary layer of AMTEX was usually low; for example, the average value of $V_0 \cdot \nabla T_0$ shown in Table I is only about 0.37 °C/hr. This is much lower than the diurnal heating rates $\partial T_0/\partial t$ commonly observed in the mid-morning hours over land. Therefore, mechanical extrainment was probably also playing a role. Its effect may be examined on the basis of Tennekes's (1973) interpolation formula (4). Because BM is a minor term compared to AH, as a first approximation for the purpose of regression analysis, the value of B obtained in previous studies may be adopted. The laboratory experiments of Kato and Phillips (1969), in the absence of convective entrainment, yielded $B = 2.5$. Subsequently, Kantha *et al.* (1977) found that their own entrainment values were approximately twice as large as those of Kato and Phillips; this led Driedonks (1982) to assume that $B = 5$ in Tennekes's interpolation formula (4). With $B = 5$, Table II indicates that BM is on average of the order of 7 or 8, which is indeed smaller than the other terms in (8) with (13). Therefore, $B = 5$ and $B/A = 20$ were used in the regression analysis. Thus, (8) with (4) and (13) can again be put in the form of (19) but the variables are defined as $X_1 = \rho_0 h(c_p V \cdot \nabla\theta + L_e V \cdot \nabla q_a) + Q_R - LE(1-\beta) - (\Delta q - s\,\Delta h)\beta L_e H/(\Delta\theta c_p) - BM$; $X_2 = H$; $X_3 =$

TABLE IV

Results of regression analyses for first-order model with Equations (8), (4), and (13)

Data	$A(\pm\sigma)$	$A_2(\pm\sigma)$	Correlation coefficients		
			Multiple	Partial	
			$R_{1.23}$	$R_{12.3}$	$R_{13.2}$
Ryofu and Keifu	0.32 (±0.16)	0.58 (±0.25)	0.83	0.83	0.41
All 3 ships	0.27 (±0.26)	0.20 (±0.39)	0.45	0.45	0.15
All data w/out No. 21	0.34 (±0.23)	0.39 (±0.35)	0.55	0.55	0.24

$(\Delta q - s\Delta h)L_e(H + BM/A)/(\Delta\theta c_p)$; $a_{12} = 1 + A$, and $a_{13} = A_2$. The results are given in Table IV. The convective entrainment constant for sensible heat, A, is reduced somewhat to about 0.3 which is more in line with the generally accepted value. The entrainment constant A_2 is again a little larger than A, but in view of the magnitudes of the standard errors, there is no good reason for not concluding that $A_2 = A$. The correlation coefficients are practically the same as those in Table III.

TABLE V

Results of regression analyses for zero-order model with Equations (8), (3), and (17)

Data	$A(\pm\sigma)$	$A_3(\pm\sigma)$	Correlation coefficients		
			Multiple	Partial	
			$R_{1.23}$	$R_{12.3}$	$R_{13.2}$
Ryofu and Keifu	−0.04 (±0.23)	0.92 (±0.34)	0.80	0.80	0.39
All 3 ships	−0.12 (±0.32)	0.58 (±0.46)	0.37	0.37	0.23
All data w/out No. 21	−0.08 (±0.30)	0.71 (±0.44)	0.45	0.45	0.27

Table V shows the results of the data analysis with the zero-order approach. The budget equation is (8) with (3) and (15). Therefore, the regression could be carried out as for Table III but with Δh taken as zero. The results show that A is very small or even negative, and that A_3 is almost certainly different from A. Since in the derivation of (15) A_3 should in fact be A, it is clear that the zero-order model is incapable of describing the present data. Similar results were obtained by including mechanical entrainment in the formulation, i.e., (18), as for Table IV but with $\Delta h = 0$. Therefore, these results are not given.

6. Discussion

The data used in the present analysis were subject to considerable errors. This was especially so in the case of the advective terms $V\cdot\nabla\theta$ and $V\cdot\nabla q_a$, which are the main

driving terms (see Table II) of the budget equations. The horizontal gradients were determined from an irregular array of shipboard, island, and coastal observations; the shipboard measurements were sometimes of dubious quality, and the small island and coastal stations often involved systematic errors on account of the land surface and other local advection effects. In addition, the near-surface wind velocity and potential temperature gradients were assumed to represent the average values for the entire boundary layer; the specific humidity gradient was assumed to obey self-similarity. On the other hand, the surface evaporation rate LE, the surface turbulent heat flux H, the values of the thickness h and Δh, and the jumps in specific humidity Δq and potential temperature $\Delta\theta$, were probably relatively accurate, say within 10%. The radiation term values are rough approximations, but Q_R is a minor term. Nevertheless, in spite of the possibly large errors involved, the relatively large correlation coefficients still inspire some confidence in the results.

One of the findings is that $A_3 > A$ or that $A_4 > A$. This can be interpreted to indicate that the zero-order model cannot be used with the present data. An alternative interpretation, as suggested at the end of Section 3, is that the ratio of the eddy diffusivities is not unity, but $(K_H/K_E) < 1$ for the stable conditions of the atmosphere at the lower boundary of the inversion layer. This can be seen directly by taking the ratio of the fluxes as given by (3) and (17). Coincidentally or not, a value of K_H smaller than that of K_E is in agreement with experiments reported by Lang *et al.* (1983) for stable conditions in the surface sublayer. These authors found that K_H/K_E is about unity for near-neutral conditions, and that it becomes as small as 0.65 with increasing stability. This result is also in qualitative agreement with that predicted by Warhaft's (1976) equation. Using data on $\overline{\theta' q'}$ published by Wyngaard *et al.* (1978) and on $\overline{w'^2}$, $\overline{\theta'^2}$, and $\overline{q'^2}$ by Lenschow *et al.* (1980), together with mean values of $\Delta\theta$, Δq, and Δh of Table I, one can readily calculate that Warhaft's (1976) equation produces a ratio K_H/K_E of about 0.5. Nevertheless, the present results shown in Table V for A_3/A_1 imply that K_H/K_E near the inversion is much smaller than values observed previously in the surface sublayer.

7. Concluding remarks

An analysis of experimental data, regarding nearly steady convection in an advective boundary layer over a sea surface within the simple framework of a slab approach, has produced the following main results. The entrainment flux for sensible heat could be taken to be proportional to the surface flux H, and the entrainment constant A was found to lie within the general range of values previously reported for other weakly convective situations in the literature, i.e., around 0.4 to 0.6. The inclusion of mechanical entrainment, in the form of Tennekes's (1973) interpolation formula did not improve the correlation (see Table V). This was probably due to the fact that additional variables may cause additional noise even if the representation of the mechanisms is improved. Nevertheless, the inclusion of mechanical entrainment resulted in values of A even closer to the consensus of 0.2 to 0.3. The water vapor flux at the top of the mixed layer could be described well on the basis of a proposed first-order model, as an extension of the

version of Betts (1974) and Deardorff (1979) for sensible heat. The main support for this is the fact that the entrainment constant for sensible heat [A_1 in (12) or A_2 in (13)] used in this approach was not found to be substantially different from A. In contrast, the zero-order model as represented by (14) did not appear suitable to describe the water-vapor fluxes through the inversion; the constants A_3 in (17) and A_4 in (18) were found to be substantially different from A. The main reason for the failure of the zero-order approach is undoubtedly the large thickness Δh of the inversion layer during AMTEX.

Acknowledgements

I would like to express my gratitude to Professor Junsei Kondo for providing some of the data (notably the near-surface temperature and humidity data) from his own files on past AMTEX studies, and for numerous discussions on this problem during my stay at Tohoku University in Sendai, Japan. I would also like to thank my colleagues Dr William P. Kustas and Dr Zellman Warhaft for helpful suggestions.

The support of this work was provided in part by the U.S. National Science Foundation through Grants No. ATM 8115713, No. ATM 8601115, and also No. INT 823639.

References

Artaz, M.-A. and André, J.-C.: 1980, 'Similarity Studies of Entrainment in Convective Mixed Layers', *Boundary-Layer Meteorol.* **19**, 51–66.

Ball, F. K.: 1960, 'Control of Inversion Height by Surface Heating', *Quart. J. Roy. Meteorol.* **86**, 483–494.

Betts, A. K.: 1973, 'Non-Precipitating Cumulus Convection and its Parameterization', *Quart. J. Roy. Meteorol. Soc.* **99**, 178–196.

Betts, A. K.: 1974, 'Reply', *Quart. J. Roy. Meteorol. Soc.* **100**, 469–471.

Carson, D. J.: 1973a, 'The Development of a Dry Inversion-Capped Convectively Unstable Boundary Layer', *Quart. J. Roy. Meteorol. Soc.* **99**, 450–467.

Carson, D. J.: 1973b, 'A Model for the Development of a Convectively Unstable Boundary Layer', *Quart. J. Roy. Meteorol. Soc.* **99**, 774–775.

Coulman, C. E.: 1978, 'Boundary-Layer Evolution and Nocturnal Inversion Dispersal, Part II', *Boundary-Layer Meteorol.* **14**, 493–513.

Deardorff, J. W.: 1979, 'Prediction of Convective Mixed-Layer Entrainment for Realistic Capping Inversion Structure', *J. Atmos. Sci.* **36**, 424–436.

Driedonks, A. G. M.: 1982, 'Models and Observations of the Growth of the Atmospheric Boundary Layer', *Boundary-Layer Meteorol.* **23**, 283–306.

Dubloscard, G.: 1980, 'A Comparison between Observed and Predicted Values for the Entrainment Coefficient in the Planetary Boundary Layer', *Boundary-Layer Meteorol.* **18**, 473–483.

Grossman, R. L.: 1982, 'An Analysis of Vertical Velocity Spectra Obtained in the BOMEX Fair-Weather, Trade-Wind Boundary Layer', *Boundary-Layer Meteorol.* **23**, 323–357.

Heidt, F. D.: 1977, 'The Growth of the Mixed Layer in a Stratified Fluid Due to Penetrative Convection', *Boundary-Layer Meteorol.* **12**, 439–461.

Kaimal, J. C., Wyngaard, J. C., Haugen, D. A., Coté, O. R., Izumi, Y., Caughey, S. J., and Readings, C. J.: 1976, 'Turbulence Structure in the Convective Boundary Layer', *J. Atmos. Sci.* **33**, 2152–2169.

Kantha, L. H., Phillips, O. M., and Azad, R. S.: 1977, 'On Turbulent Entrainment at a Stable Density Interface', *J. Fluid. Mech.* **79**, 753–768.

Kato, H. and Phillips, O. M.: 1969, 'On the Penetration of a Turbulent Layer into Stratified Fluid', *J. Fluid. Mech.* **37**, 643–665.

Kondo, J.: 1976, 'Heat Balance of the East China Sea During the Air Mass Transformation Experiment', *J. Meteorol. Soc. Japan* **54**, 382–398.

Kondo, J.: 1977, 'Geostrophic Drag and the Cross-Isobar Angle of the Surface Wind in a Baroclinic Convective Boundary Layer over the Ocean', *J. Meteorol. Soc. Japan* **55**, 301–311.

Lang, A. R. G., McNaughton, K. G., Chen, F., Bradley, E. F., and Ohtaki, E.: 1983, 'Inequality of Eddy Transfer Coefficients for Vertical Transport of Sensible and Latent Heats During Advective Inversions', *Boundary-Layer Meteorol.* **25**, 25–41.

Lenschow, D. H. and Agee, E. M.: 1974, 'The Air Mass Transformation Experiment (AMTEX): Preliminary Results from 1974 and Plans for 1975', *Bull. Amer. Meteorol. Soc.* **55**, 1228–1235.

Lenschow, D. H. and Agee, E. M.: 1976, 'Preliminary Results from the Air Mass Transformation Experiment (AMTEX), *Bull. Amer. Meteorol. Soc.* **57**, 1346–1355.

Lenschow, D. H. and Stephens, P. L.: 1980, 'The Role of Thermals in the Convective Boundary Layer', *Boundary-Layer Meteorol.* **19**, 509–532.

Lenschow, D. H., Wyngaard, J. C., and Pennell, W. T.: 1980, 'Mean Field and Second Moment Budgets in a Baroclinic, Convective Boundary Layer', *J. Atmos. Sci.* **37**, 1313–1326.

Lilly, D. K.: 1968, 'Models of Cloud-Topped Mixed Layers Under a Strong Inversion', *Quart. J. Roy. Meteorol. Soc.* **94**, 292–309.

Mahrt, L.: 1976, 'Mixed Layer Moisture Structure', *Mon. Weather Rev.* **104**, 1403–1418.

Mahrt, L. and Paumier, J.: 1984, 'Heat Transport in the Atmospheric Boundary Layer', *J. Atmos. Sci.* **41**, 3061–3075.

Manton, M. J.: 1977, 'On the Structure of Convection', *Boundary-Layer Meteorol.* **12**, 491–503.

Murty, L. Krishna: 1976, 'Heat and Moisture Budgets over AMTEX Area During AMTEX '75', *J. Meteorol. Soc. Japan* **54**, 370–381.

Ninomiya, K.: 1974, 'Note on Synoptic Situation and Heat Energy Budget During AMTEX '74', *J. Meteorol. Soc. Japan* **52**, 452–455.

Nimoiya, K.: 1977, 'Heat Energy Budget of the Polar Air-Mass Transformed over Kuroshio Region Under the Situation of Strong Subsidence', *J. Meteorol. Soc. Japan* **55**, 431–441.

Nitta, T.: 1976, 'Large-Scale Heat and Moisture Budgets During the Air Mass Transformation Experiment', *J. Meteorol. Soc. Japan* **54**, 1–14.

Stull, R. B.: 1976, 'The Energetics of Entrainment Across a Density Interface', *J. Atmos. Sci.* **33**, 1260–1278.

Taconet, O. and Weill, A.: 1983, 'Convective Plumes in the Atmospheric Boundary Layer as Observed with an Acoustic Doppler Sodar', *Boundary-Layer Meteorol.* **25**, 143–158.

Tennekes, H.: 1973, 'A Model for the Dynamics of the Inversion Above a Convective Boundary Layer', *J. Atmos. Sci.* **30**, 558–567.

Warhaft, Z.: 1976, 'Heat and Moisture Flux in the Stratified Boundary Layer', *Quart. J. Roy. Meteorol. Soc.* **102**, 703–707.

Wyngaard, J. C., Pennell, W. T., Lenschow, D. H., and LeMone, M. A.: 1978, 'The Temperature-Humidity Covariance Budget in the Convective Boundary Layer', *J. Atmos. Sci.* **35**, 47–58.